

LATE CRETACEOUS ARC AND BACK-ARC FORMATION WITHIN THE SOUTHERN NEOTETHYS: WHOLE-ROCK, TRACE ELEMENT AND Sr-Nd-Pb ISOTOPIC DATA FROM BASALTIC ROCKS OF THE YÜKSEKOVA COMPLEX (MALATYA- ELAZIĞ, SE TURKEY)

Melek Ural*, Mehmet Arslan**, M. Cemal Göncüoğlu***,✉, U. Kagan Tekin° and Sevcan Kürüm*

* Department of Geological Engineering, Fırat University, Elazığ, Turkey.

** Department of Geological Engineering, Karadeniz Technical University, Trabzon, Turkey.

*** Department of Geological Engineering, Middle East Technical University, Ankara, Turkey.

° Department of Geological Engineering, Hacettepe University, Beytepe, Ankara, Turkey.

✉ Corresponding author, e-mail: mcgoncu@metu.edu.tr

Keywords: *mélange basalts, petrology, arc-back arc, Southern Neotethys.*

ABSTRACT

The remnants of the Southern Neotethys are represented by ophiolitic bodies and subduction/accretion complexes along the Southeast Anatolian-Zagros suture belt in the Eastern Mediterranean. Around Malatya and Elazığ areas (SE Turkey), they are found within imbricated slices of a *mélange* complex, known as the Yüksekova Complex. The studied basaltic rocks are common members of this *mélange* complex, and show distinctive features of sources with tholeiitic to tholeiitic-transitional character. Petrography, whole-rock trace element and isotopic data reveal two different compositional groups. Group I is transitional between island arc tholeiites and normal mid-ocean ridge basalt, and Group II includes back-arc (BABB), enriched mid-ocean ridge (E-MORB), and ocean island basalt type (OIB) compositions. According to the known Late Cretaceous stratigraphic ages, the studied basaltic rocks have $(^{87}\text{Sr}/^{86}\text{Sr})_i = 0.703666-0.706394$, $(^{143}\text{Nd}/^{144}\text{Nd})_i = 0.512734-0.512927$, $^{208}\text{Pb}/^{204}\text{Pb} = 38.3216-39.3400$, $^{207}\text{Pb}/^{204}\text{Pb} = 15.5018-15.6262$ and $^{206}\text{Pb}/^{204}\text{Pb} = 18.5655-19.3209$. In addition, ϵNd_i values vary between +3.99 and +8.01 with two-stage T_{DM} values ranging from 0.25 to 0.59 Ga. In the Sr versus Nd isotope correlation diagram, most samples plot along the mantle array line. In the correlation diagrams of $^{206}\text{Pb}/^{204}\text{Pb}$ versus $^{208}\text{Pb}/^{206}\text{Pb}$ and $^{207}\text{Pb}/^{206}\text{Pb}$, the rock samples also plot nearly on the Northern Hemisphere Reference Line, similar to Atlantic and Pacific Ocean ridge basalts. As a whole, the isotopic data reveal that the studied rocks were derived from a depleted mantle source.

When plotted in the conventional tectonic discrimination diagrams based on immobile trace elements, the samples can be related to an arc environment (Group I basalts), and back arc basin (Group II basalts) developed by generation and maturation of the rifted arc in later stages. This interpretation is supported by ages obtained from pillow lava-radiolarian chert associations indicating that the arc stage was realized during the late Cenomanian-early Turonian, followed by Coniacian-early Maastrichtian spreading in a back arc basin within the closing southern branch of Neotethys.

INTRODUCTION

The representatives of the southern Neotethyan (*sensu* Sengör and Yılmaz, 1981) oceanic lithosphere are observed today as a distinct belt of ophiolites and ophiolitic *mélanges* that can be followed from the Troodos Mountains in Cyprus via SE Anatolia to Zagros Mountains and Oman in the East (Figs. 1 and 2). They were formed during the closure of the Southern Neotethys Ocean at the end of Mesozoic and Early Tertiary (e.g., Robertson, 2002; 2004; Robertson et al., 2007; Göncüoğlu et al., 2015). Ongoing compression along the suture during the Tertiary resulted in a thick pile of nappes that include oceanic assemblages together with variably metamorphosed units belonging to the conjugate continental margins of this ocean (e.g., Göncüoğlu et al., 1997).

Within this belt, the *mélange* complexes are geographically distributed to the north and south of an E-W trending zone of metamorphic massifs (e.g., Göncüoğlu and Turhan, 1984) including the Pütürge and Bitlis metamorphic massifs (Fig. 2) in Turkey. From these, the *mélanges* to the north of the metamorphic zone are collectively named as the Yüksekova Complex (Perincek, 1979). Available data on the geochemistry of the volcanic rocks within the Yüksekova Complex suggests on the whole a “supra-subduction-type” oceanic crust generation (e.g., Parlak et al., 2004; 2009). However, the tectonic setting of the volcanic rocks within the supra-subduction zone is not well constrained. Moreover, very few data on their formation ages are available.

In this study we present new petrographic, whole-rock petrochemical and Sr-Nd-Pb isotopic data for the Yüksekova Complex basaltic rocks within the Malatya and Elazığ-Palu segment from the northern belt of Southern Neotethys. Our aim is to better-understand their petrogenesis, evaluate the nature of their source region and to assess their geodynamic setting.

GEOLOGICAL FRAMEWORK

In SE Anatolia, between the Mediterranean Sea in the west and the Iran-Iraq border in the east, disrupted bodies of oceanic lithosphere origin were already recognised in the earliest tectonic models (e.g., Sengör and Yılmaz, 1981). They form a nappe-stack, several km-thick, between the Malatya-Keban Metamorphics of the Tauride-Anatolide terrane in the north and the Bitlis-Pütürge Metamorphics of the Arabian Plate in the South. Within this suture belt, distinct bodies with ophiolitic stratigraphy were separately described and named as Göksun, Berit, Ispendere, Kömürhan and Guleman Ophiolites (e.g., Bingöl, 1984). The *mélange* complexes around Hakkari, on the other hand, were initially included in the “Yüksekova Complex”, by Perincek (1979). By definition, the Yüksekova Complex represents an accretional complex and comprises allochthonous bodies derived from an intra-oceanic arc that developed within the Late Mesozoic southern Neotethys oceanic branch. Around

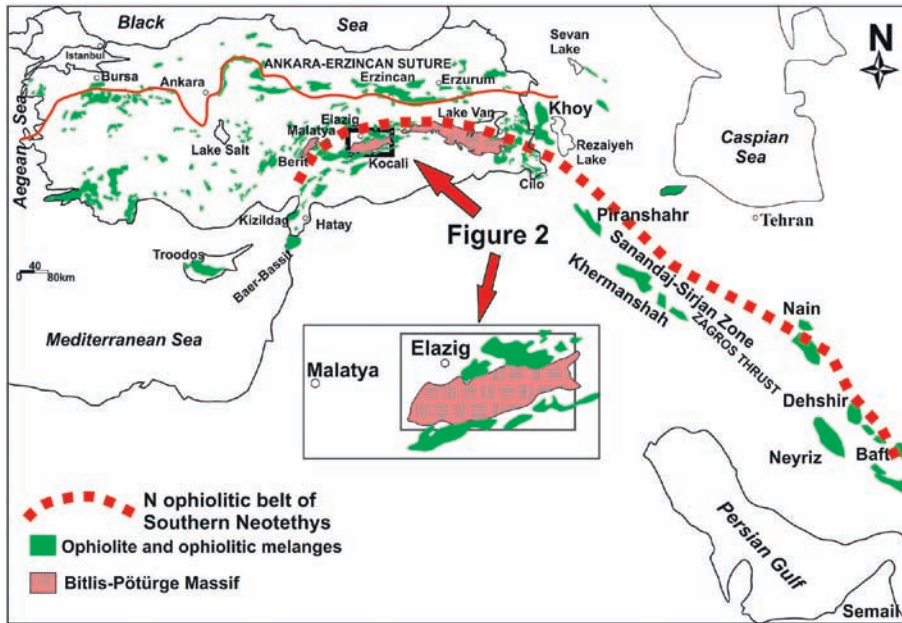


Fig. 1 - Distribution of the ophiolites and mélangé complexes in the Eastern Mediterranean and location of the study area (after Göncüoğlu, 2014).

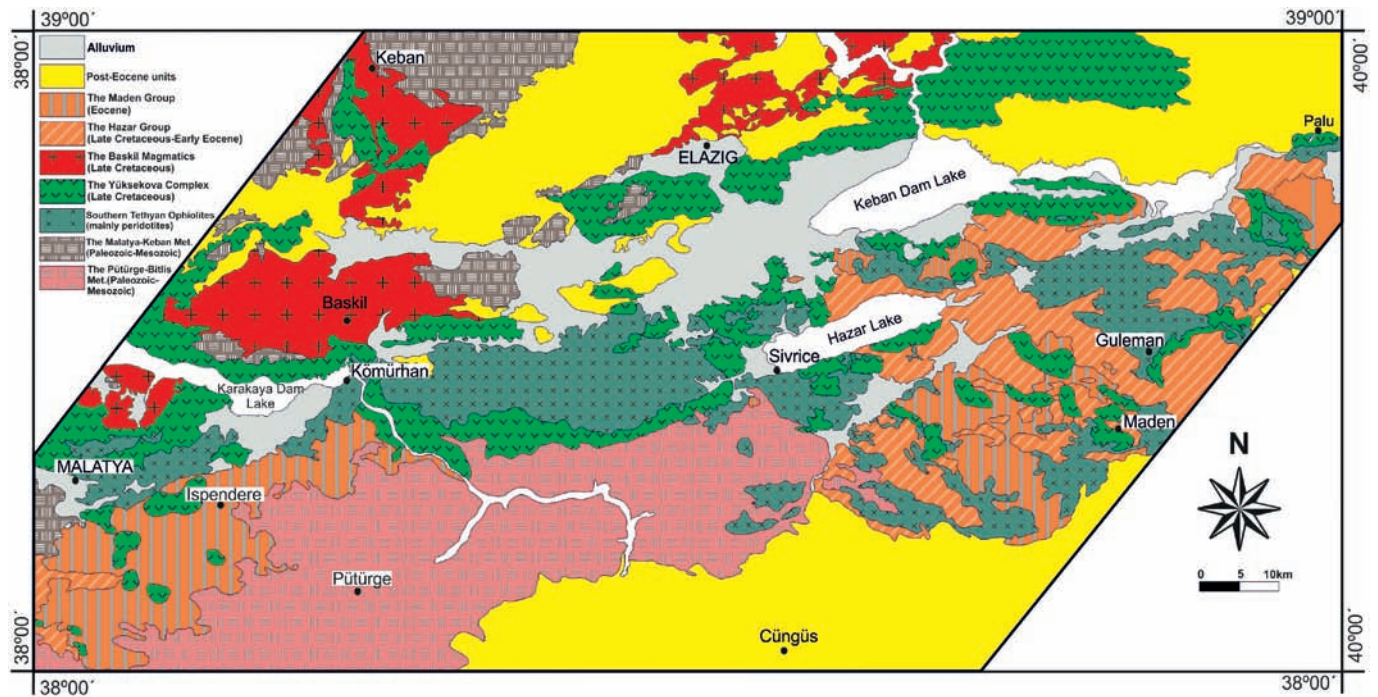


Fig. 2 - Geological map showing the distribution of the main oceanic and continental units in the area between cities of Malatya and Elazığ in SE Turkey (after MTA, 2002).

Elazığ, the same name has been used by several authors (e.g., Naz, 1979; Perincek and Özkaya, 1981; Bingöl, 1984; Perincek and Kozlu, 1984; Sungurlu et al., 1985; Turan and Bingöl, 1991) for the mélangé complexes. However, there are others (e.g., Bingöl, 1982; Özkan, 1983; Aktas and Robertson, 1984; 1990; Hempton, 1984; Bingöl and Beyarslan, 1996) who have used a number of different names for the same mélangé unit.

The Yüksekova Complex is made of an assemblage of slide-blocks (Fig. 3), with different sizes and lithologies. The blocks consist of red-green limestones, shales, greywackes, tuffs, agglomerates, basalts, diabases, gabbros and serpentinites. They are enclosed in a sedimentary matrix

comprising shales, coarse-grained sandstones, pebbly-mudstones and pebbly-sandstones. The size of the basalt blocks within the mélangé varies in size from a few meters to several hundreds of square meters. The most common blocks are pillow lavas with intra-pillow radiolarian cherts and mudstones. The pillow lavas are variably altered and cut by diabase dykes. They include calcite- and zeolite-filled vesicles at the rim of the pillows.

Individual chert and/or micritic limestone sequences within the volcanic-volcanoclastic units are up to 3-m thick, brick to red-violet in colour and may comprise dm-thick radiolarian cherts alternating with micritic limestones and green-red mudstones. The intra-pillow cherts and radiolarian



Fig. 3 - a) General view of the Yüksekova Complex with blocks of serpentinites, pillow-lavas, diabase dykes and radiolarian cherts at Kinederiç ramp on the Elazığ-Sivrice highway, b) Blocks of pillow lavas to the NW of Maden town, c) Blocks with pillow-lavas, dykes, mudstones N of Caybağı village, d) Close-up view of pillow lavas and radiolarian cherts in depositional contact in Yaygın village (SW of Malatya). C- radiolarian cherts; D- dykes; M- red-violet mudstones; P- pillow-lavas; S- serpentinites.

cherts between pillow-lava horizons have been studied in detail by Tekin et al. (2015). Two distinct ages are recognized as late Cenomanian-early Turonian and early Coniacian-early Maastrichtian based on the characteristic radiolarian assemblages (Fig. 4). The older ages are restricted to the Group I basalts that will be described in the following chapters, whereas the younger ones are only found in cherts associated with Group II basalts.

The Yüksekova Complex is intruded by granitic rocks, known as the Baskil Magmatics (for a recent evaluation see Rizaoglu et al., 2009). The name was originally used for the granitic rocks intruding the Yüksekova Complex together with the structurally overlying low-grade metamorphic Paleozoic-Mesozoic successions of the Malatya-Keban unit of the Tauride-Anatolide terrane (Yazgan, 1984). The radiometric ages obtained from the Baskil Magmatics range between 85-82 Ma (Karaoglan et al., 2013) which put an upper age limit for the mélangé formation. The oldest sedimentary cover disconformably overlying the Yüksekova Complex is the Hazar Group of late Maastrichtian age, which provides another constraint for the maximum age of the mélangé formation.

ANALYTICAL METHODS

A total of 212 samples were collected from the area between Malatya and Elazığ cities in SE Turkey (Fig. 5). An optical microscope study was carried out to determine textural-mineralogical features of the collected samples, and to select the freshest samples for geochemical analyses, in order to overcome the most severe seafloor/hydrothermal alteration effects. Among samples examined under the polar-

izing microscope, a total of 175 samples from pillow basalt (115 samples), massive basalt (52 samples), and sub-volcanic rocks (8 samples) were chosen and analysed for whole-rock major, trace and rare earth elements (REE) at ACME Analytical Laboratory (Vancouver, Canada). Samples were crushed into small chips using a jaw crusher and then pulverized using a mild-steel mill. Major and trace element compositions were determined by inductively coupled plasma atomic emission spectroscopy (ICP-AES) from pulp after 0.2 g of rock powder was fused with 1.5 g LiBO_4 and then dissolved in 100 mL of 5% HNO_3 . The REE contents were analyzed by inductively coupled plasma mass spectrometry (ICP-MS) after 0.25 g of rock powder samples were fused and then dissolved by acid digestion steps. The detection limits range from 0.01 to 0.1 wt% for major oxides, 0.1 to 10 ppm for trace elements, and 0.01 to 0.5 ppm for the REE.

The Sr and Nd isotope geochemical measurements were performed by TRITON Thermal Ionization Mass Spectrometer (Thermo-Fisher) at the Radiogenic Isotope Laboratory in METU Central Laboratories (Ankara, Turkey), following the procedure described in Köksal and Göncüoğlu (2008). Uncertainties are in 2 sigma level. The Pb isotopes were measured by multi-collector inductively coupled plasma mass spectrometry (MC-ICP-MS) at Pacific Centre for Isotopic and Geochemical Research (PCIGR), Department of Earth and Ocean Sciences the Earth and Oceanic Sciences, University of British Columbia (Vancouver, Canada). The reference values are from Weiss et al. (2005; 2006). The NBS 981 standard and normalization values are 36.7219 for $^{208}\text{Pb}/^{204}\text{Pb}$, 15.4963 for $^{207}\text{Pb}/^{204}\text{Pb}$ and 16.9405 for $^{206}\text{Pb}/^{204}\text{Pb}$.

| | | Sample 09-SIV-5 | Sample 09-SC-3 | Sample 09-KV-4 | Sample 09-MDN-1 | Sample 09-MDN-2 | Sample 09-MDN-3 | Sample 09-SIV-9 | Sample 09-US-8 | |
|-------------------------------|---------------|--|--|---|---|---|---|---|--|--|
| | | <i>Patellula verteroensis</i> <i>Ps. pseudomacrocephala</i> <i>Pseudodictyonitra tiara</i> <i>Thanaria veneta</i> <i>Dictyonitra formosa</i> | <i>Patellula verteroensis</i> <i>Ps. pseudomacrocephala</i> <i>Pseudodictyonitra tiara</i> | <i>Alievium gallowayi</i> <i>Patellula verteroensis</i> <i>Dictyonitra koslovae</i> | <i>Dictyonitra formosa</i> <i>Dictyonitra koslovae</i> | <i>Alievium superbum</i> <i>Pseudoaulophacus floresensis</i> <i>Pseudoaulophacus lenticulatus</i> <i>Pseudoaulophacus pargueraensis</i> <i>Dictyonitra koslovae</i> | <i>Dictyonitra formosa</i> <i>Dictyonitra koslovae</i> | <i>Alievium gallowayi</i> <i>Pseudoaulophacus lenticulatus</i> <i>Patellula verteroensis</i> <i>Dictyonitra formosa</i> <i>Dictyonitra koslovae</i> | <i>Patellula verteroensis</i> <i>Dictyonitra koslovae</i> | |
| U P P E R C R E T A C E O U S | Maastrichtian | U | | | | | | | | |
| | | L | | | | | | | | |
| | Campanian | U | | | | | | | | |
| | | M | | | | | | | | |
| | | L | | | | | | | | |
| | | U | | | | | | | | |
| | San. | U | | | | | | | | |
| | | L | | | | | | | | |
| | | U | | | | | | | | |
| | | L | | | | | | | | |
| | Turonian | U | | | | | | | | |
| | | L | | | | | | | | |
| U | | | | | | | | | | |
| L | | | | | | | | | | |
| Coniacian | U | | | | | | | | | |
| | L | | | | | | | | | |
| | U | | | | | | | | | |
| | L | | | | | | | | | |
| Cenomanian | U | | | | | | | | | |
| | L | | | | | | | | | |
| | U | | | | | | | | | |
| | L | | | | | | | | | |

Fig. 4 - Age ranges of the radiolarian cherts and micritic limestones associated with the Group I and Group II basalts from the Yüksekova Complex in the Malatya and Elazığ areas (simplified after Tekin et al., 2015).

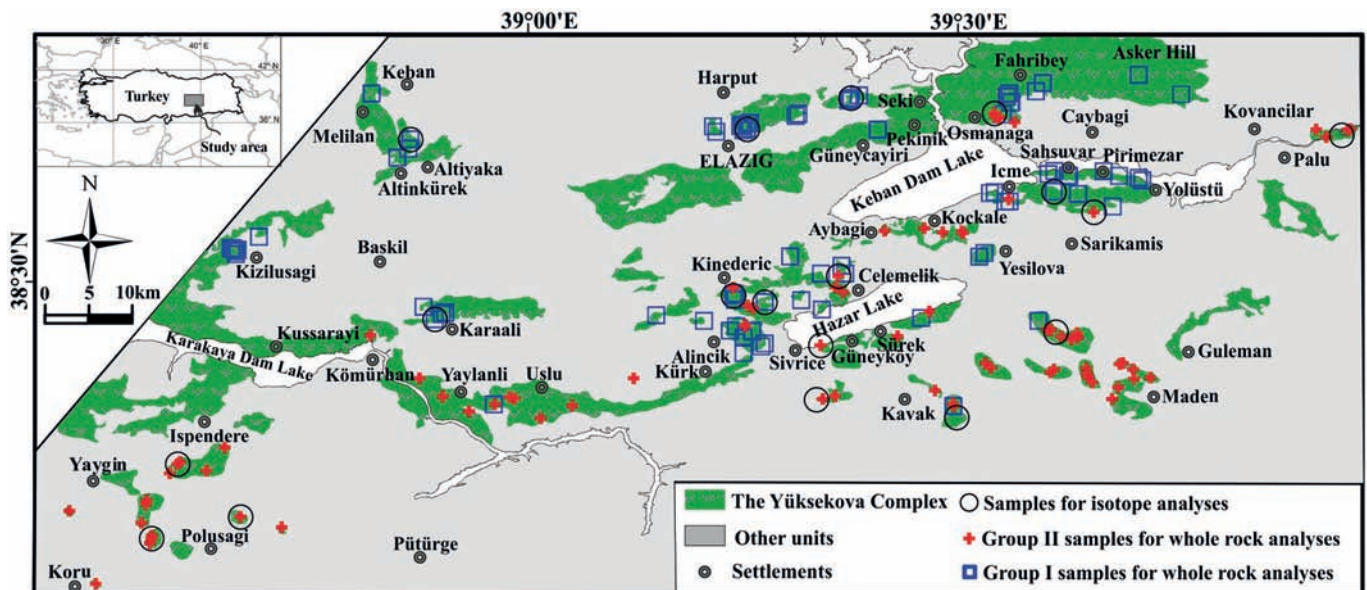


Fig. 5 - Distribution of basaltic rock samples taken from the Yüksekova Complex between cities of Malatya and Elazığ in SE Turkey.

RESULTS

Petrography

The majority of Late Cretaceous massive and pillow basic volcanic and sub-volcanic rocks outcropping around Malatya and Elazığ regions (Fig. 6) have similar mineralogical and

textural features. In detail, however, two distinct groups can be identified on the basis of their phenocryst assemblage. Group I samples are mainly pyroxene- and plagioclase-phyric, while Group II samples contain pyroxene and plagioclase together with olivine. Generally, both Group I and II rocks show variable degrees of sea-floor/hydrothermal

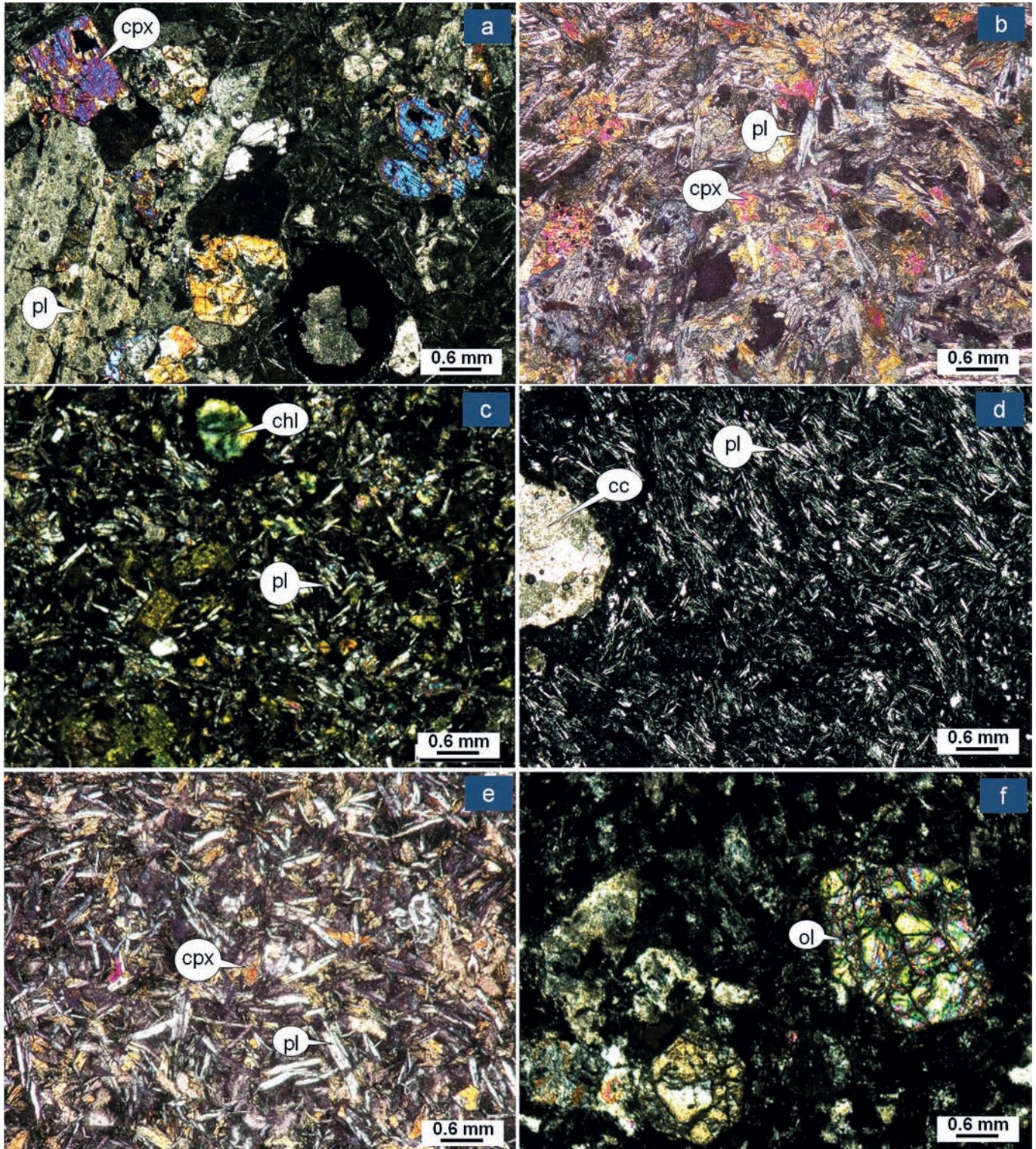


Fig. 6 - Microphotographs of the basaltic rock samples from the Yüksekova Complex. a) glomeroporphyritic basalt sample with clinopyroxene and plagioclase phenocrysts (Caybağı, CB-21; Group I); b) clinopyroxene-phyric basalt (pillow lava) sample with doleritic texture (Sivrice, SIV-5b; Group I); c) massive basalt sample showing chloritization (North of Hazar Lake; SC-1; Group I); d) amigdaloidal basalt sample with fluidal texture (Palu, PA-3; Group II); e) variolitic texture in clinopyroxene-phyric basalt sample (Pütürge, PT-3; Group II); f) partly serpentinized olivine phenocrysts in olivine-phyric basalt sample (Maden, MD-13; Group II), (crossed nicols; pl- plagioclase, cpx- clinopyroxene, ol- olivine, cc- calcite, chl- chlorite).

alteration with formation of sericite, epidote, chlorite and carbonates.

Group I and II rocks are basalts showing microlitic, microlitic porphyric, hyalo-microlitic, hyalo-microlitic porphyric, amigdaloidal, variolitic, glomeroporphyric textures. Some volcanic and sub-volcanic rock samples from both groups show intersertal, intergranular and rarely sub-ophitic textures (Fig. 6).

Group I and II samples contain mainly plagioclase and lesser amounts of ortho- and clinopyroxenes and hornblende. However, olivine (both as phenocrysts and in the groundmass) is only observed in Group II samples. In both Group I and II, the rocks locally include clusters of opaque minerals (up to 30-35%). Plagioclase is frequently altered, as evidenced by its optically measured composition, variable between An_5 to An_{32} . In Group II rocks, the olivine show variable degree of serpentinization. Relatively fresh pyroxenes and olivines are only observed as relict phases. In both groups, pyroxenes are generally subhedral, sometimes completely altered to actinolite and/or iron oxide by uraltization. Hornblende is variably replaced by chlorite.

Whole-rock geochemistry

Major oxide and trace element analyses of the basaltic rocks are presented in Appendix in the journal web page (<http://www.ofioliti.it/index.php/ofioliti/article/view/435>). In terms of some major oxide and trace element content, the examined rocks generally show a limited compositional range, excepting the samples affected by hydrothermal alteration and/or ocean floor metamorphism. These variations are also consistent with the degree of alteration of the studied rocks. Evidence for alteration effect on the studied rocks also comes from variable loss on ignition (LOI) values ranging between 1.40-14.80 wt% for Group I and 3-11.5 wt% for Group II rocks (see Appendix), which is corroborated by the presence of a considerable amount of water- and/or carbon dioxide-bearing minerals such as chlorite, serpentine, and calcite observed in thin section. Group I rocks have 34.4-52.0 wt% SiO_2 and 0.46-1.54 wt% TiO_2 . Group II rocks have 39.2-51.9 wt% SiO_2 and 0.58-2.16 wt% TiO_2 . In both Group I and II rocks, the highly variable concentrations of some major oxides such as Na_2O (0.02-7.46 wt%), K_2O (0.01-6.16 wt%), CaO (1.99-25.20 wt%) and MgO (1.68-11.58 wt%) indicate that many rocks have undergone seafloor alteration (e.g., Frey and Weis, 1995; Gillis, 1995). Besides, the large ion lithophile elements (LILEs) are relatively mobile during underwater volcanic eruptions and post-magmatic alteration (Humphris and Thompson, 1978). However, trace elements such as Zr, Y, Nb, Ni, Ti, V, Cr and rare-earth elements are usually considered to be immobile and appear to remain largely unaffected by hydrothermal alteration and/or ocean floor metamorphism (e.g., Winchester and Floyd, 1976; Wood, 1980; Rollinson, 1993). Geochemical and tectonic discrimination of the studied rocks was therefore realized by using the immobile trace elements mentioned above.

Petrochemically, the studied basaltic rocks display two distinct groups which are compatible with their discrimination based upon their ages and petrography. Collectively, based on chemical nomenclature plot by using the Nb/Y vs. $Zr/TiO_2 * 0.0001$ immobile element diagram of Winchester and Floyd (1977) revised by Pearce (1996), all basaltic rock samples from the Yüsekova Complex plot in basalt field (Fig. 7a). Besides, all the samples are characterized by

relatively low Nb/Y ratios (0.02-0.18 for Group I and 0.05-1.08 for Group II), plotting in the field of subalkaline basalt. The geochemical affinities of the studied basaltic rocks were determined by using Zr vs. Y and La vs. Yb immobile element binary plots of Ross and Bédard (2009). Overall, Group I samples show mainly tholeiitic and Group II samples exhibit dominantly tholeiitic-transitional character (Fig. 7b and c).

In major and trace element variation plots vs. Zr (Fig. 8), CaO, MgO, Cr and Ni indicate negative correlations whereas TiO_2 , Hf and Y exhibit a positive correlation for both Group I and II (Fig. 8). These variations may be explained by fractionation of mafic phases (pyroxene ± olivine) in the evolution of the studied rocks. Besides, Zr versus Th and Nb plots (Fig. 8) discriminate two group of rocks.

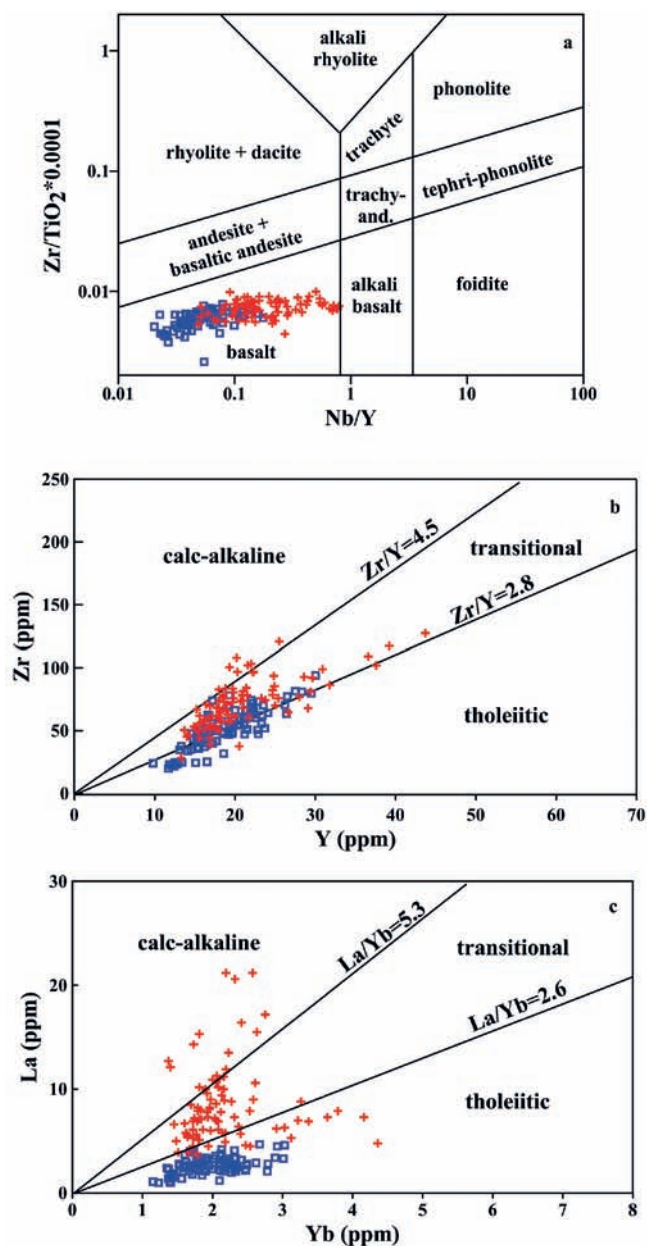


Fig. 7 - a) Chemical nomenclature based on the Nb/Y vs. $Zr/TiO_2 * 0.0001$ immobile element diagram of Winchester and Floyd (1977) revised by Pearce (1996), b) Y vs. Zr and c) Yb vs. La geochemical affinity plots of Barrett and MacLean (1999) revised by Ross and Bédard (2009) for the basaltic rocks from the Yüsekova Complex. For symbols see Fig. 5.

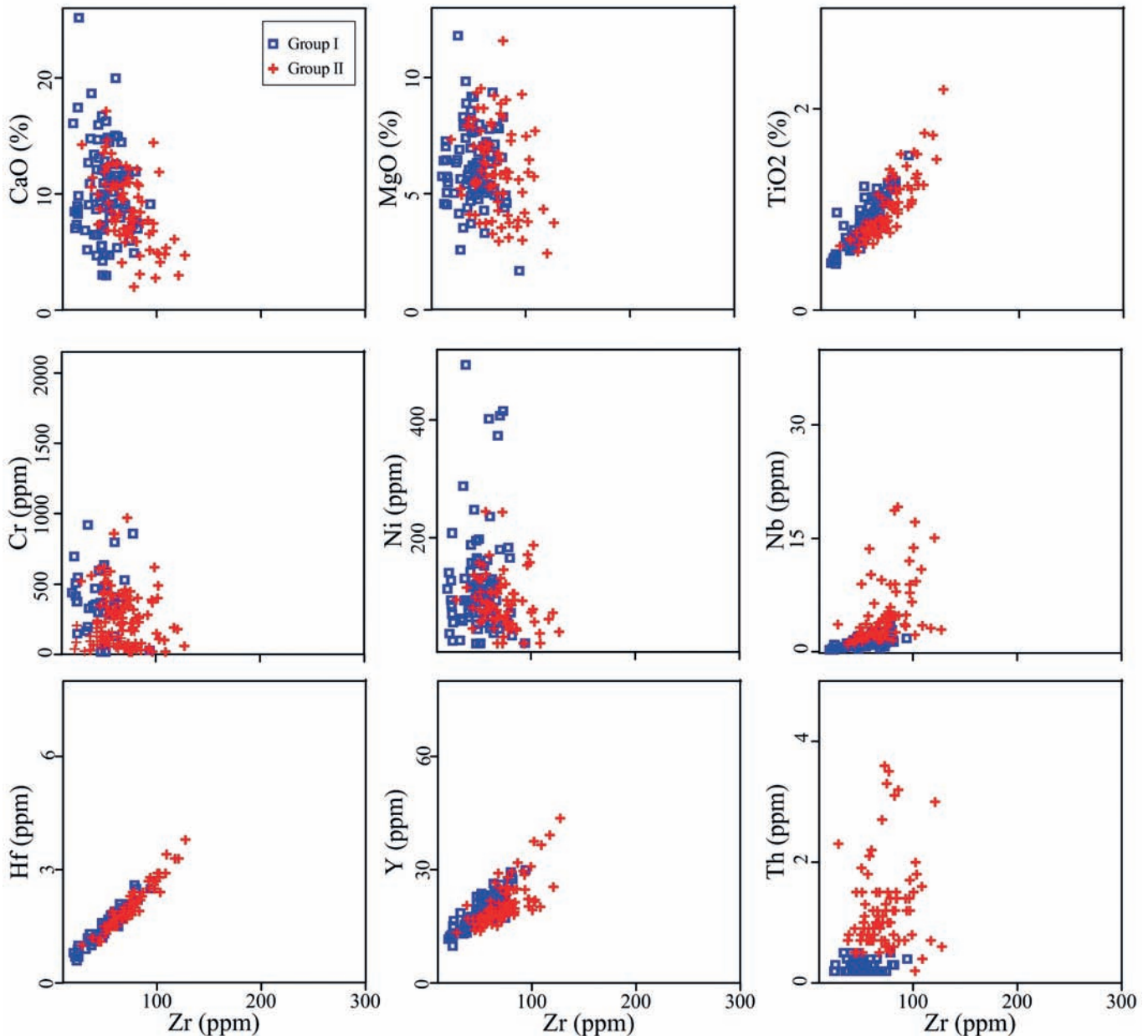


Fig. 8 - Selected major and trace element vs. Zr variation diagrams for the basaltic rocks from the Yüsekova Complex.

N-MORB normalized incompatible element diagrams (Fig. 9a and c) show variable enrichments and depletions in LILE (e.g., K, Rb, Ba and Sr). However, N-MORB normalized immobile HFSE (e.g., Nb, Hf, Zr, Y) reveal more distinctive variation with more depleted patterns for Group I, compared to those of Group II (Fig. 9a and c). Almost all the rock samples are enriched in Th but Nb shows both positive and negative anomalies. Ti and Y remain almost at the level of the N-MORB but Ti show no significant enrichment compared to Y for the studied rocks. Generally, Group I rocks show significant negative Nb anomalies but Group II rocks show positive Nb anomalies. Besides, N-MORB normalized patterns of Group II shows relative enrichment in Nb compared to those of Group I (Fig. 9c). Overall, N-MORB normalized HFSE patterns of the rocks show two types of patterns, indicating that Group I is comparable with island arc tholeiite (IAT) whereas Group II includes E-MORB-like compositions (Fig. 9a and c).

Chondrite-normalized REE variations of the studied rocks reveal two distinctive types of patterns (Fig. 9b and d). Group I rocks show LREE-depleted to nearly flat patterns with $La_N/Lu_N = 0.38-1.71$, $La_N/Yb_N = 0.41-1.74$ and $Eu_N/Eu^* = 1.03-1.50$. Group II rocks exhibit flat to enriched LREE, with $La_N/Lu_N = 0.76-7.10$, $La_N/Yb_N = 0.79-6.94$ and $Eu_N/Eu^* = 1.02-1.47$. The absence of negative Eu anomalies in the studied rocks suggests no significant fractionation of plagioclase. However, positive Eu anomalies in some samples can be explained by plagioclase accumulation and/or Eu mobility due to hydrothermal alteration. Furthermore, in terms of LREE enrichment relative to HREE, Group I rocks are characterized by depleted to nearly flat LREE between N- and E-MORB with $La_N/Sm_N = 0.39-1.38$ whereas Group II rocks have slightly depleted to enriched LREE between E-MORB and OIB compositions with $La_N/Sm_N = 0.84-3.87$ (Fig. 9b and d; see Appendix).

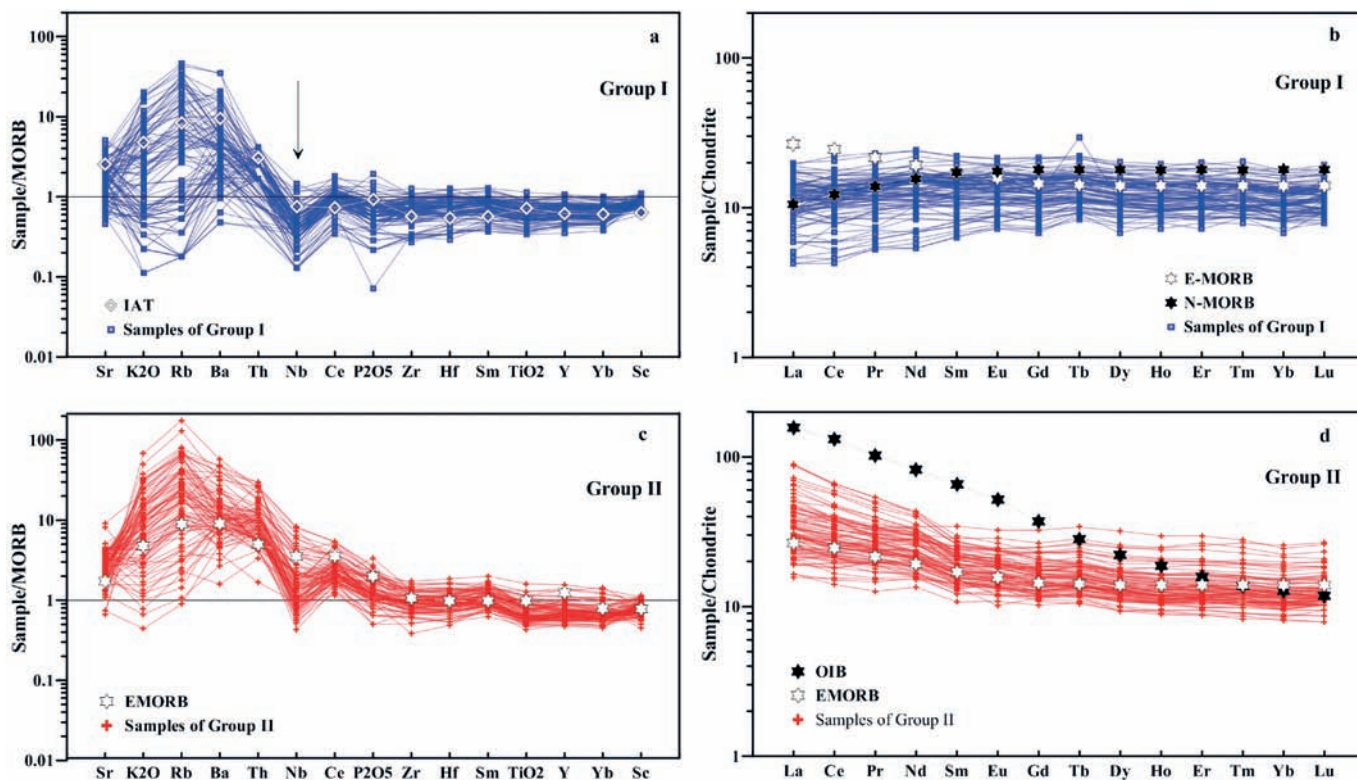


Fig. 9 - N-type MORB normalized multi-element and chondrite-normalized REE patterns for Group I (a, b) and Group II (c, d) basaltic rocks from the Yüsekova Complex. Compositions of island arc tholeiite (IAT), ocean island basalt (OIB), enriched-mid ocean ridge basalt (E-MORB) and normal-mid ocean ridge basalt (N-MORB) were also plotted for comparison. Normalization values and compositions used for comparison are from Pearce (1983) and Sun and Mc Donough (1989).

Sr-Nd-Pb Isotope Compositions

Sr-, Nd- and Pb-isotope data of the studied basaltic rocks are presented in Table 1. While the measured Sr-isotope data in the studied rocks are slightly variable ranging from 0.703748 to 0.708227, Nd- and Pb-isotopic data show a narrow range. The initial isotopic compositions were calculated to 94 Ma for Group I and 84 Ma for Group II samples based on the stratigraphic and radiolarian ages (see Fig. 4). $(^{87}\text{Sr}/^{86}\text{Sr})_i$ values range from 0.703781 to 0.705403 for Group I rocks, and from 0.703666 to 0.706394 for Group II rocks. ϵNd_i values of the studied rocks are between +4.47 and +8.01 for Group I; between +3.99 and +6.51 for Group II rocks. $^{208}\text{Pb}/^{204}\text{Pb}$ values are between 38.3216 and 38.8495 (Group I), 38.6790 and 39.3400 (Group II); $^{207}\text{Pb}/^{204}\text{Pb}$ values are between 15.5018 and 15.6262 (Group I), 15.5611 and 15.6174 (Group II), $^{206}\text{Pb}/^{204}\text{Pb}$ values are between 18.5655 and 19.1357 (Group I), 18.8204 and 19.3209 (Group II). In addition, two-stage T_{DM} values are between 0.25 and 0.56 Ga for Group I, 0.37 and 0.59 Ga for Group II rocks.

DISCUSSION

Source characteristics

The trace element patterns of the studied rocks (massive/pillow basaltic and sub-volcanic rock samples) within Group I are subparallel. Besides, HFSE in the rocks are similar to MORB or a little more enriched than MORB (see Fig. 9a and c). Therefore, Group I rocks have a transitional character between IAT and N-MORB. Group II rocks have

BABB, OIB and E-MORB like compositions. Group I and BABB type basalts of Group II, show nearly horizontal patterns, excepting for Nb, suggesting that the rocks evolved from a melt or melts similar to N-MORB. E-MORB and OIB-type basalts of Group II, however, may have been derived from more enriched sources. Although subduction-related signatures dominate in back-arc basins, E-MORB and OIB-like basaltic rocks may also occur in back-arc basins (Saunders and Tarney 1984; Aldanmaz et al., 2008). Besides, changes in fractionation of HREE may reflect mantle source having suffered different degrees of partial melting (Beccaluva and Serri, 1988).

In the chondrite-normalized REE diagrams of the studied basaltic rocks, there are two distinctive patterns with low and moderate enrichments for Group I and Group II, respectively (see Fig. 9b and d). However, differences in level of enrichment within the same group may be related to remelting of a depleted source or to the distance from the axis of the arc, during the rifting. Besides, the Nd and Pb isotopic compositions of the two rock groups (see Table 1) show a similar range of variation, suggesting similar mantle sources. The data points to a depleted mantle source where ϵNd_i values of both groups are positive, although some deviations from DM values towards more enriched compositions are also observed.

In the Nd versus Sr isotope correlation diagram (Fig. 10a), most samples plot along the mantle array line. Shifting towards higher initial $^{87}\text{Sr}/^{86}\text{Sr}$ ratios most likely reflects addition of more radiogenic Sr from seawater and/or during post-magmatic alteration. Furthermore, in the Nd vs Pb isotope correlation diagram (Fig. 10b), the two rock

Table 1 - Sr-, Nd- and Pb-isotope analysis of Group I and Group II basaltic rocks of Yütksekovalı Complex around Elazığ and Malatya.

| Sample | Sr (ppm) | Rb (ppm) | $^{87}\text{Rb}/^{86}\text{Sr}$ | $^{87}\text{Sr}/^{86}\text{Sr}$ | ϵ_{Sr} | $(^{87}\text{Sr}/^{86}\text{Sr})_i$ | Sm (ppm) | Nd (ppm) | $^{147}\text{Sm}/^{144}\text{Nd}$ | $^{143}\text{Nd}/^{144}\text{Nd}$ | ϵ_{Nd} | $(^{143}\text{Nd}/^{144}\text{Nd})_i$ | ϵ_{Nd} | $^{208}\text{Pb}/^{204}\text{Pb}$ | ϵ_{Pb} | $^{207}\text{Pb}/^{204}\text{Pb}$ | ϵ_{Pb} | $^{206}\text{Pb}/^{204}\text{Pb}$ | ϵ_{Pb} | $T_{\text{DM}}^*(\text{Ga})$ | $T_{\text{DM}}^*(\text{Ga})$ |
|-----------------|----------|----------|---------------------------------|---------------------------------|------------------------|-------------------------------------|----------|----------|-----------------------------------|-----------------------------------|------------------------|---------------------------------------|------------------------|-----------------------------------|------------------------|-----------------------------------|------------------------|-----------------------------------|------------------------|------------------------------|------------------------------|
| Group I | | | | | | | | | | | | | | | | | | | | | |
| ALC-8 | 115.4 | 0.2 | 0.005013 | 0.704524 | 18 | 0.704517 | 6.4 | 21.1 | 0.183964 | 0.512958 | 18 | 0.512845 | 6.40 | 38.3978 | 26 | 15.5069 | 9 | 18.5656 | 9 | 0.989 | 0.391 |
| CU-4 | 94.9 | 0.9 | 0.027433 | 0.705354 | 5 | 0.705317 | 2.2 | 6.1 | 0.218054 | 0.51288 | 30 | 0.512746 | 4.47 | 38.5939 | 16 | 15.5648 | 6 | 18.8223 | 8 | -9.825 | 0.558 |
| HPS-2 | 161.7 | 12 | 0.214645 | 0.704378 | 6 | 0.704091 | 3.1 | 10.3 | 0.183735 | 0.513011 | 6 | 0.512898 | 7.43 | 38.6771 | 25 | 15.5893 | 8 | 18.7973 | 9 | 0.713 | 0.300 |
| KNM-2 | 163.5 | 0.3 | 0.005307 | 0.703788 | 18 | 0.703781 | 2.5 | 7 | 0.215939 | 0.513037 | 14 | 0.512904 | 7.55 | 38.8495 | 19 | 15.5778 | 7 | 19.1357 | 8 | -7.992 | 0.290 |
| KS-6 | 152.3 | 4 | 0.075973 | 0.705504 | 7 | 0.705403 | 1.84 | 4.8 | 0.231776 | 0.51307 | 32 | 0.512927 | 8.01 | 38.6843 | 21 | 15.6262 | 8 | 18.8284 | 8 | -0.687 | 0.250 |
| MD-5 | 135.9 | 19.1 | 0.406513 | 0.704646 | 12 | 0.704103 | 5.4 | 18.5 | 0.176481 | 0.512926 | 29 | 0.512817 | 5.86 | 38.544 | 21 | 15.5248 | 7 | 18.8878 | 9 | 0.922 | 0.437 |
| MDN-6 | 93.7 | 1.8 | 0.055569 | 0.705467 | 13 | 0.705393 | 6.8 | 20.4 | 0.202131 | 0.512937 | 17 | 0.512813 | 5.77 | 38.431 | 27 | 15.5018 | 9 | 18.5655 | 9 | 2.802 | 0.445 |
| PK-3 | 261 | 0.5 | 0.005541 | 0.705184 | 5 | 0.705177 | 1.61 | 4.6 | 0.211612 | 0.512888 | 16 | 0.512758 | 4.70 | 38.5883 | 20 | 15.5657 | 7 | 18.8103 | 7 | 18.143 | 0.538 |
| SC-3 | 129 | 10.9 | 0.244418 | 0.705478 | 8 | 0.705152 | 2.6 | 6 | 0.217661 | 0.51294 | 9 | 0.512806 | 5.64 | 38.3216 | 32 | 15.5375 | 7 | 18.6116 | 9 | -8.370 | 0.456 |
| SIV-2 | 96.5 | 9.5 | 0.284740 | 0.704423 | 9 | 0.704043 | 2.08 | 6.3 | 0.199619 | 0.512957 | 42 | 0.512834 | 6.19 | 38.7344 | 32 | 15.5629 | 12 | 19.012 | 13 | 2.092 | 0.409 |
| Group II | | | | | | | | | | | | | | | | | | | | | |
| ALC-6 | 66.5 | 35.3 | 1.535916 | 0.708227 | 18 | 0.706394 | 2.6 | 9 | 0.172649 | 0.512895 | 15 | 0.512800 | 5.27 | 38.7531 | 15 | 15.6174 | 6 | 18.8204 | 7 | 0.951 | 0.480 |
| CB-26 | 105.9 | 0.6 | 0.016387 | 0.704551 | 7 | 0.704531 | 1.6 | 6.3 | 0.157392 | 0.51295 | 15 | 0.512864 | 6.51 | 38.8333 | 20 | 15.5961 | 7 | 19.0459 | 9 | 0.545 | 0.373 |
| IS-4 | 124 | 16 | 0.373214 | 0.704606 | 6 | 0.704161 | 3.29 | 14.6 | 0.136241 | 0.512823 | 30 | 0.512748 | 4.26 | 38.9413 | 32 | 15.5922 | 14 | 19.3209 | 15 | 0.646 | 0.568 |
| PA-3 | 514.2 | 7.9 | 0.044437 | 0.704413 | 6 | 0.704360 | 3.27 | 14.2 | 0.139231 | 0.512932 | 32 | 0.512855 | 6.35 | 38.9255 | 19 | 15.5982 | 7 | 19.1719 | 8 | 0.449 | 0.386 |
| PL-5 | 154.4 | 9 | 0.168593 | 0.704246 | 8 | 0.704045 | 2.92 | 9.7 | 0.182006 | 0.512909 | 15 | 0.512809 | 5.45 | 38.7822 | 23 | 15.5812 | 8 | 19.143 | 9 | 1.163 | 0.465 |
| PT-3 | 240.8 | 5.7 | 0.068461 | 0.703748 | 6 | 0.703666 | 3.41 | 15.4 | 0.133877 | 0.512883 | 7 | 0.512809 | 5.45 | 38.9831 | 17 | 15.6017 | 6 | 19.2873 | 8 | 0.513 | 0.464 |
| SP-2 | 267 | 9.5 | 0.102928 | 0.706094 | 5 | 0.705971 | 2.29 | 10.6 | 0.130615 | 0.512806 | 15 | 0.512734 | 3.99 | 39.34 | 36 | 15.5961 | 13 | 19.2866 | 15 | 0.634 | 0.592 |
| SRK-3 | 173.9 | 14 | 0.232855 | 0.704576 | 5 | 0.704298 | 2.91 | 10.8 | 0.162908 | 0.512877 | 25 | 0.512787 | 5.03 | 38.679 | 21 | 15.5611 | 7 | 18.9479 | 8 | 0.823 | 0.502 |

Note: According to the stratigraphic age accepted as the average 94 Ma (Group I) and 84 Ma (Group II), corrections in Sr and Nd isotopic compositions of the examined rocks is calculated with the formulas $\{(^{87}\text{Sr}/^{86}\text{Sr})_i = (^{87}\text{Sr}/^{86}\text{Sr})_0 - [(^{87}\text{Rb}/^{86}\text{Sr})_0 - 1] \cdot e^{\lambda t}\}$, $(^{143}\text{Nd}/^{144}\text{Nd})_i = (^{143}\text{Nd}/^{144}\text{Nd})_0 - [(^{147}\text{Sm}/^{144}\text{Nd})_0 - 1] \cdot e^{\lambda t}\}$ (Faure, 2001; Faure and Mensing, 2005).

$\lambda(^{87}\text{Rb}) = 1.42 \times 10^{-11} \text{ y}^{-1}$; $\lambda(^{147}\text{Sm}) = 6.54 \times 10^{-12} \text{ y}^{-1}$; t : million age.

Calculated values of ϵ_{Sr} , ϵ_{Nd} and T_{DM} (model age) is calculated using the following formulas: $\epsilon_{\text{Sr}} = (^{87}\text{Sr}/^{86}\text{Sr})_{\text{sample}} / (^{87}\text{Sr}/^{86}\text{Sr})_{\text{CHUR}} - 1$; $\epsilon_{\text{Nd}} = (^{143}\text{Nd}/^{144}\text{Nd})_{\text{sample}} / (^{143}\text{Nd}/^{144}\text{Nd})_{\text{CHUR}} - 1$;

$T_{\text{DM}} = (1/\lambda) \times \ln \{ [(^{143}\text{Nd}/^{144}\text{Nd})_{\text{sample}} - 0.513151] / [(^{147}\text{Sm}/^{144}\text{Nd})_{\text{sample}} - 0.2137] + 1 \}$ (Faure, 2001; Faure and Mensing, 2005).

CHUR: Chondritic Uniform Reservoir; DM: Depleted Mantle. $T_{\text{DM}}^*(\text{Ga})$: single stage model age. $T_{\text{DM}}^{**}(\text{Ga})$: two stage model age.

groups fall close and/or within MORB fields, corroborating the hypothesis of a depleted mantle source, with no significant role for a crustal contribution. A slight change in source is possible for the Group II rocks that were developed in back arc setting. Depleted asthenospheric mantle is likely metasomatized by the fluids/melts derived from the subducted slab. In the correlation diagrams of $^{206}\text{Pb}/^{204}\text{Pb}$ versus $^{208}\text{Pb}/^{204}\text{Pb}$ (Fig. 10c), the rock samples plot on the Northern Hemisphere Reference Line, similar to Atlantic and Pacific MORBs, which implies derivation from a depleted mantle source and the possible involvement of a HIMU component.

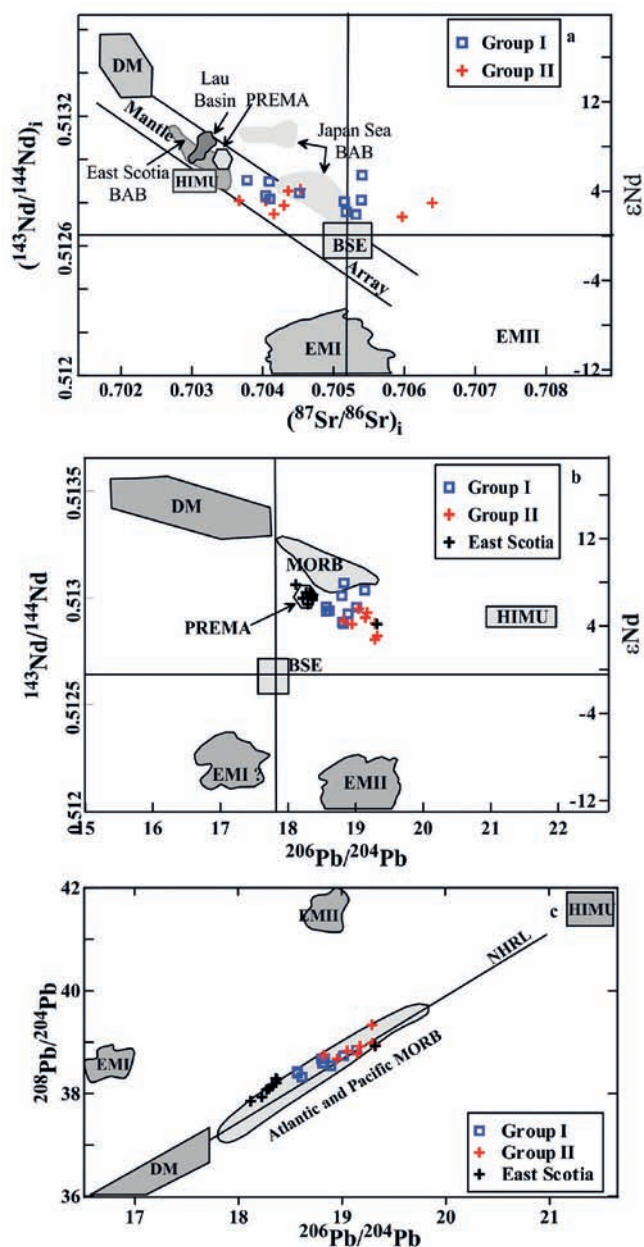


Fig. 10 - a) $(^{87}\text{Sr}/^{86}\text{Sr})_i$ vs. $(^{143}\text{Nd}/^{144}\text{Nd})_i$, b) and c) $(^{206}\text{Pb}/^{204}\text{Pb})$ vs. $(^{143}\text{Nd}/^{144}\text{Nd})$ and $(^{208}\text{Pb}/^{204}\text{Pb})$ isotope correlation diagrams for the basaltic rocks from the Yüksekova Complex. (BSE- Bulk Silicate Earth; DM- Depleted Mantle; EMI, EMII- Enriched mantle; HIMU- High μ ; PREMA- Prevalent Mantle; MORB- mid-ocean ridge basalt [Mantle reservoirs defined by Zindler and Hart (1986) are taken from Rollinson (1993) and Faure (2001); Lau basin (Tian et al., 2008); Japan Sea BABB (Nohda et al., 1992), East Scotia Ridge BAB (Leat et al., 2000).

The effects of fractional crystallization and/or degree of source enrichment on the evolution of the studied rocks are suggested by selected major and trace element variations (e.g., Fig. 8). In the variation diagrams, some immobile major and trace element variations display positive or negative correlations with increasing Zr contents, reflecting the role of fractional crystallization processes during the evolution of the studied rocks. Furthermore, $(^{87}\text{Sr}/^{86}\text{Sr})_i$ versus Rb/Sr, Th and Sr, and $(^{143}\text{Nd}/^{144}\text{Nd})_i$ versus Nd and Sm/Nd plots (Fig. 11) show almost horizontal trends, indicating no signatures for significant continental crust contamination or mixing. Note that assimilation by crustal material within the magma chamber or enroute to the surface would hardly lead to the coupled enrichment in highly incompatible mobile LILE (e.g., Rb) on one hand and the negative Nb-Ta-Ti anomalies on the other hand (e.g., Pearce and Peate, 1995).

Tectonic discrimination and geodynamic implications

The geologic-tectonic evolution of the studied basaltic rocks can be reconstructed by using tectono-magmatic discrimination diagrams (e.g., Rollinson, 1993). Numerous bivariate, ternary and multidimensional tectonic discrimination plots are available for ultrabasic and basic volcanic rocks (e.g., Pearce and Cann, 1971; 1973; Pearce and Norry, 1979; Wood, 1980; Shervais, 1982; Meschede, 1986; Floyd et al., 1991; Saunders and Tarney, 1991; Woodhead et al., 1993; Pearce, 2008; Agrawal et al., 2008; Verma, 2010; Verma and Agrawal, 2011; Verma et al., 2012).

In Zr vs. Zr/Y (Pearce and Norry, 1979), Zr vs. V/Ti (Woodhead et al., 1993), V vs. Ti/1000 (Shervais, 1982) and Y vs. La/Nb (Floyd et al., 1991) immobile element tectonic discrimination diagrams, the basaltic rock samples from the Yüksekova Complex generally plot in the N-MORB, BABB and IAB fields (Fig. 12a and b). According to Pearce et al. (1994), the axis of spreading close to the arc-trench system is characterized by transition between N-MORB and IAT affinity for Group I rocks, whereas the dominant BABB-type character with some E-MORB and OIB-like character of Group II rocks reflects the back-arc environment as seen in Fig. 12a, b and d. According to Pearce (2008), back-arc basin basalts (BABB) may lie within the MORB-OIB array if the inflowing mantle is not influenced by the subduction component; with increasing arc proximity compositions are displaced from the MORB-OIB array. On the binary diagram of Ce/Nb-Th/Nb, samples of Group I distribute between IAT and N-MORB, however, samples of Group II show a distribution between fore-arc and back-arc (Ural et al., 2014).

Therefore, it may be suggested that subduction component contribution for the studied rocks, decreases from the Group I towards Group II. Some Group II samples are in close proximity to OIB, revealing a more enriched source. In the multidimensional tectonic discrimination diagrams (not shown here), the studied rocks plot in the transition among IAB and MORB or field of MORB in diagram of DF1-DF2 of Agrawal et al. (2008). These diagrams attest rifting of an arc environment, and subsequent back arc basin development by maturation of the rifted arc. By this, we interpret the Yüksekova basalts within the SE Anatolian suture belt as remnants of a Late Cretaceous arc-back arc system.

This interpretation diverges from the previous suggestions, where the pillow basalts around Elazığ area were variably considered as representatives of an Andean-type island

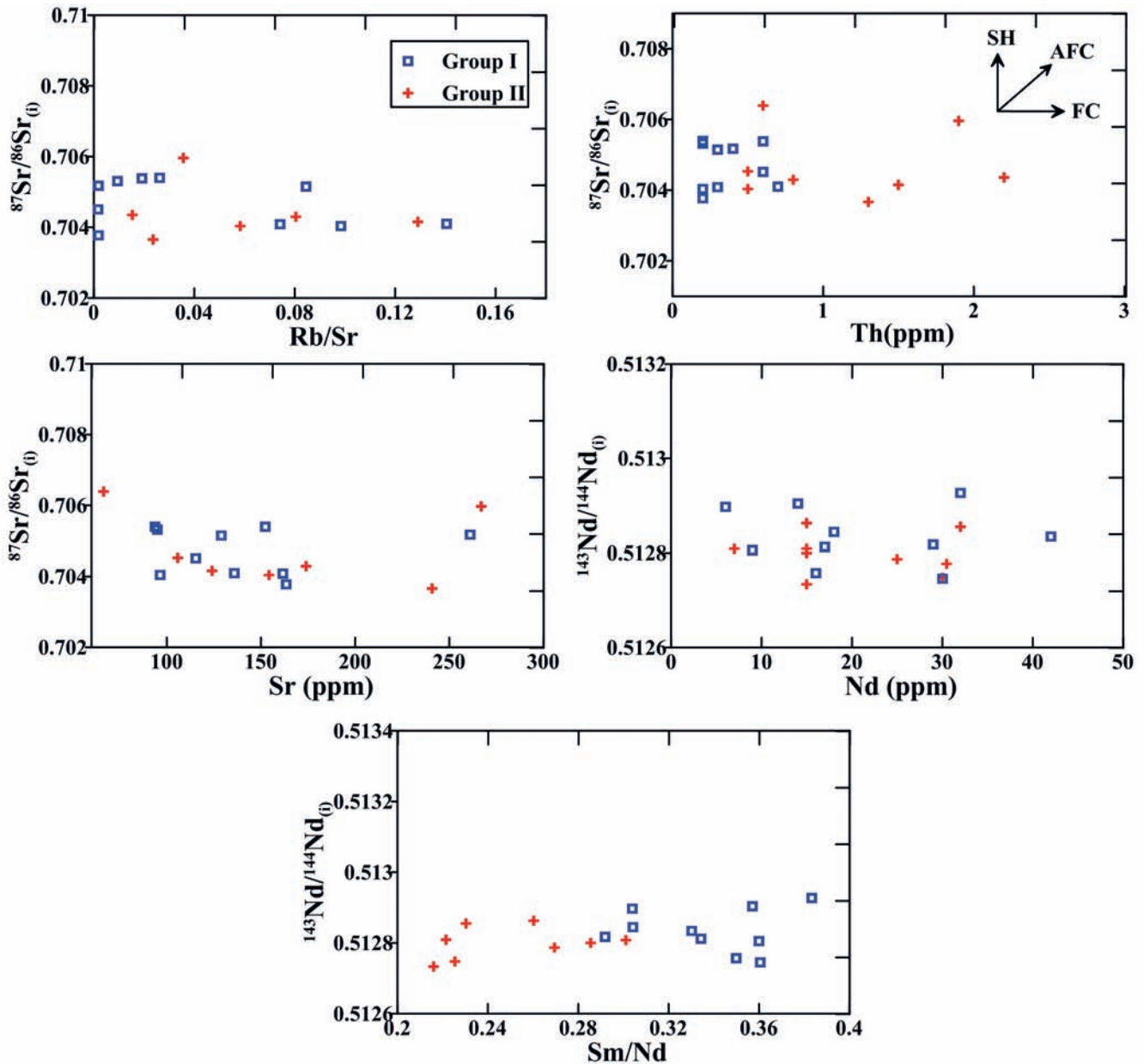


Fig. 11 - ($^{87}\text{Sr}/^{86}\text{Sr}_i$) vs. Rb/Sr, Th and Sr, and ($^{143}\text{Nd}/^{144}\text{Nd}_i$) vs. Nd and Sm/Nd correlation diagrams for the basaltic rocks from the Yüsekova Complex. FC- Fractional crystallization; AFC- Assimilation - fractional crystallization; SH- Source heterogeneities.

arc (Herece et al., 1992), an association of island-arc magmatics, tholeiitic (“ensimatic” in Beyarslan and Bingöl, 2000) island arc rocks developed during the mature stage of supra-subduction spreading (Parlak et al., 2004; 2009; Rızaoglu et al., 2006; Robertson et al., 2007) and intra-arc rocks (e.g., Bölücek et al., 2004).

When shown on a simplified cartoon (Fig. 13) within the Southern Branch of Neotethys surrounded by the Malatya-Keban units of the Tauride-Anatolide Terrane in the north and the Bitlis-Pütürge Metamorphics representing the north Arabian margin in the South, the intra-oceanic subduction first gave way to the formation of the Yüsekova island arc (Group I rocks) during the late Cenomanian-early Turonian (Fig. 13a). Actually, the earliest product of the intra-oceanic subduction should have created a new SSZ-type oceanic lithosphere, represented by the Kizildag-type fore-arc assemblages (e.g., Dilek and Thy,

2009). Yet, the fore-arc assemblages have probably emplaced earlier onto the Arabian platform-margin or dismembered and accreted into the subduction-accretion prism, as there are no boninites detected in the Malatya-Elazığ-Van segment of the SE Anatolian Suture belt to the north of the Bitlis-Pütürge Massifs. Roll-back of the old and cooled oceanic lithosphere (Fig. 13b) resulted in extension in the arc and back-arc area during the early Cretaceous and early Maastrichtian. The subduction-modified mantle rocks above the subduction are invaded by melts formed by adiabatic decompression of depleted asthenospheric mantle. This resulted in a change in the composition of the Group II rocks to E-MORB with still recognisable subduction affect. These enriched melts intruded the extending former crust in intra- and back-arc settings during the Maastrichtian (Fig. 13c) and formed the new back-arc lithosphere. The data we obtained from the study areas do

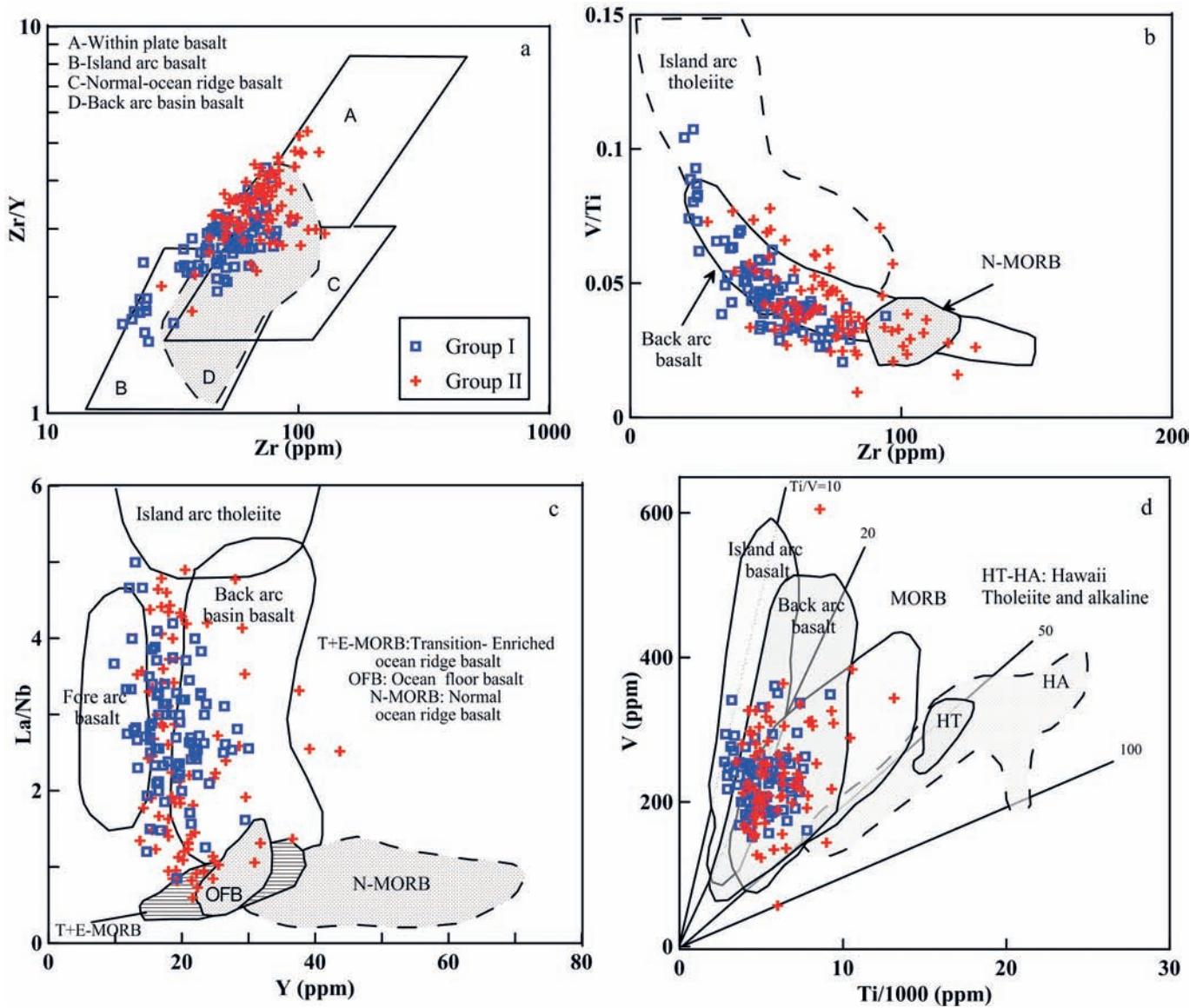


Fig. 12 - Tectonic discrimination diagrams for the basaltic rocks ($\text{SiO}_2 < 52$) from the Yüksekova Complex. a) Zr vs. Zr/Y (Pearce and Norry, 1979; revised from Floyd et al., 1991); b) Zr vs. V/Ti (Woodhead et al., 1993); c) La/Nb vs. Y (Floyd et al., 1991); d) V vs. Ti/1000 (Shervais, 1982) plots.

not allow to evaluate in detail the evolution of the Southern Neotethys during the post-Maastrichtian stage. However, regional geological interpretations (e.g., Bingöl and Beyarslan, 1996; Rizaoglu et al., 2006; Robertson et al., 2013), suggest that the northward subduction continued in the north of the studied areas to create the Baskil magmatic arc that intrude the Tauride-Anatolide platform margin, represented by the Malatya-Keban Metamorphics. From late Maastrichtian onwards all the units formed within the Southern Neotethys must have started to imbricate together with flysch-type sediments (e.g., the Hazar Group in the Elazığ area, Fig. 2) formed in small basins (e.g., Aktas and Robertson, 1984; Hempton, 1985; Yilmaz et al., 1993). The Tertiary evolution of the SE Anatolian suture belt is dominated by compressional and transtensional events (e.g., Yigitbas and Yilmaz, 1996; Robertson et al., 2013) that are out of the scope of this study.

CONCLUSIONS

In this paper we have studied the basalts in primary contact with oceanic sediments (radiolarites and radiolarian cherts) within blocks and/or gravity slices in the mélangé at the central part of the belt between Malatya and Elazığ areas. Whole-rock geochemical data, Sr-Nd-Pb isotope composition and paleontological data provided for the first time reliable data on the tectono-magmatic settings as well as formation times of two distinct events characterized by Group I and Group II basalts (see Figs. 7 and 8). Tectono-magmatic discrimination diagrams point out rifting of an arc environment, and back arc basin development by maturation of the rifted arc. Moreover, radiolarians obtained from the cherts in primary association with Group I and Group II basalts yielded late Cenomanian-early Turonian, and Coniacian-early Maastrichtian ages, respectively (Tekin et al., 2015). On this basis, we propose a scenario for the Late

Cretaceous evolution of the Southern Branch of Neotethys. As suggested by several authors (Sengör and Yilmaz, 1981; Yazgan, 1984; Göncüoğlu and Turhan, 1984; Parlak et al., 2009; Robertson et al., 2013), the scenario involves the intra-oceanic subduction of the southern Neotethyan lithosphere

there (see Fig. 13) towards north. From late Albian onwards, Kizildag-type fore-arc and arc volcanism started to form all along the subduction zone. The basalts from the Yüksekova Complex representing an arc and back arc complex were formed subsequently during middle and Late

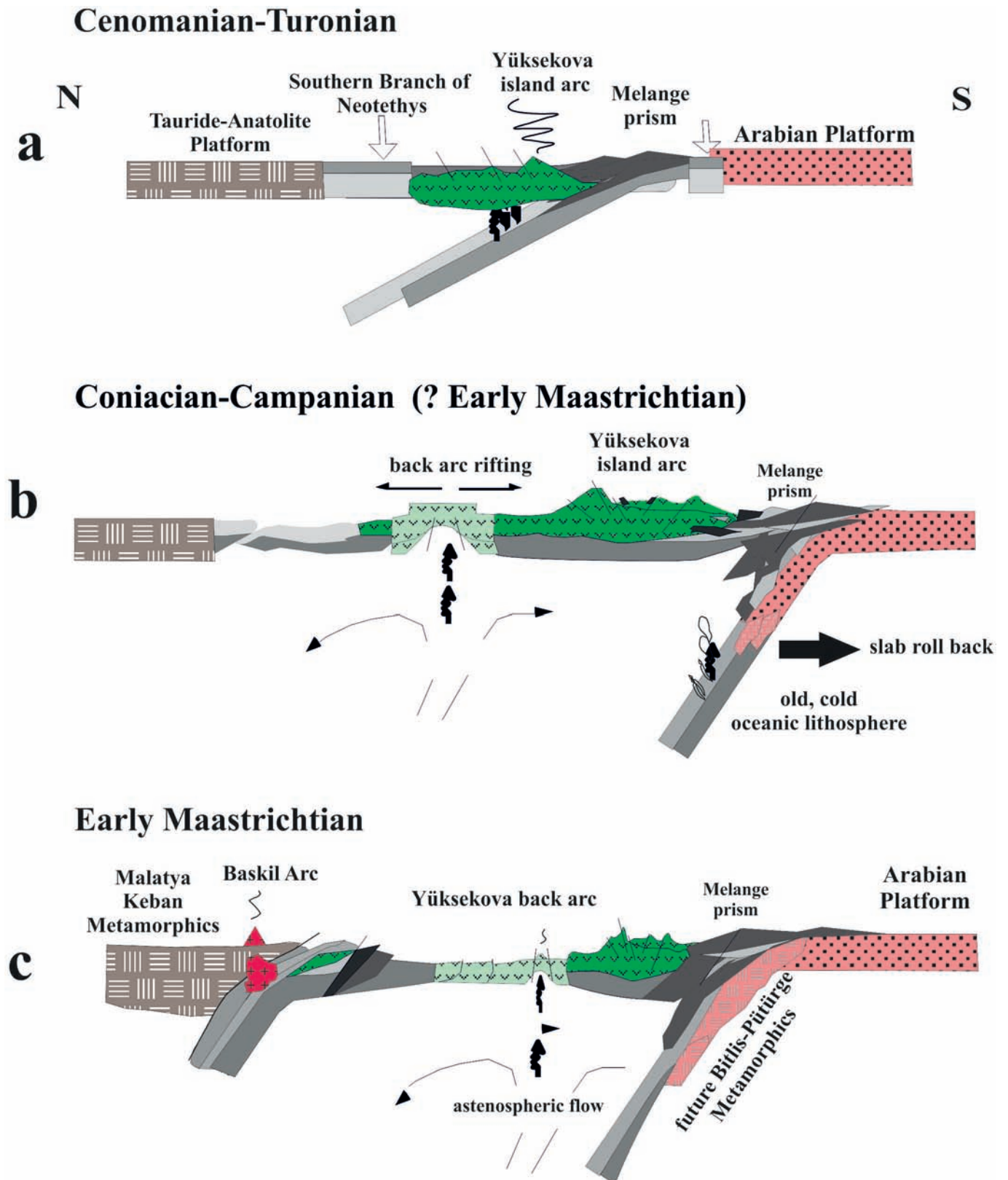


Fig. 13 - Suggested geodynamic evolution of the Southern Neotethys during the Late Cretaceous (see text for explanations).

Cretaceous (see Fig. 13). Hence, a complete system of fore-arc, arc and back-arc volcanism was formed within the closing Southern Neotethys. The youngest ages obtained for the back-arc basalts is late Maastrichtian, as recently reported from the Van area at the Iranian border (Colakoglu et al., 2012; 2014) as well as from a number of back-arc volcanics from southern Iran along the Zagros belt (e.g., Moghadam et al., 2013). Remarkably, Maastrichtian is also the time when the subduction/accretion prism material and the mélange complexes started to be emplaced towards south onto the northern continental margin of the Arabian microplate all along the Bitlis-Zagros Suture Belt.

ACKNOWLEDGEMENTS

This study was supported by the Firat University Scientific Research Fund (FUBAP-1632) and TUBITAK (108Y201). METU Central Laboratories are acknowledged for the isotope measurements. The authors gratefully acknowledge Dr. K. Sayit (METU Ankara) and two anonymous referees for their critical comments and contributions to the present manuscript.

REFERENCES

- Agrawal S., Guevara M. and Verma S.P., 2008. Tectonic discrimination of basic and ultrabasic volcanic rocks through log-transformed ratios of immobile trace elements. *Int. Geol. Rev.*, 50: 1057-1079.
- Aktas G. and Robertson A.H.F., 1984. The Maden Complex, SE Turkey: evolution of a Neotethyan active margin. In: J.E. Dixon and A.H.F. Robertson (Eds.), *The geological evolution of the Eastern Mediterranean*. Blackwell Sci. Publ., Oxford, p. 375-402.
- Aktas G. and Robertson A.H.F., 1990. Tectonic evolution of the Tethys suture zone in SE, Turkey: Evidence from the petrology and geochemistry of Late Cretaceous and Middle Eocene extrusives. In: J. Malpas et al. (Eds.), *Ophiolites - Oceanic crustal analogues*. *Proceed. Troodos Ophiolite Symp.*, Geol. Survey, Cyprus, p. 311-328.
- Aldanmaz E., Yaliniz M.K., Güctekin A. and Göncüoğlu M.C., 2008. Geochemical characteristics of mafic lavas from the Tethyan ophiolites in western Turkey: implications for heterogeneous source contribution during variable stages of oceanic crust generation. *Geol. Mag.*, 145: 37-54.
- Barrett T.J. and Mac Lean W.H., 1999. Volcanic sequences, litho-geochemistry, and hydrothermal alteration in some bimodal volcanic-associated massive sulphide systems, *Rev. Econ. Geol.*, 8: 101-113.
- Beccalova L. and Serri G., 1988. Boninitic and low-Ti subduction related lavas from intraoceanic arc-backarc systems and low-Ti ophiolites: reappraisal of their petrogenesis and original tectonic setting. *Tectonophysics*, 146: 291-315.
- Beyarslan M. and Bingöl A.F., 2000. Petrology of a supra-subduction zone ophiolite (Kömürhan- Elazığ-Turkey). *Can. J. Earth Sci.*, 37: 1411-1424.
- Bingöl A.F., 1982. Petrographic and petrologic study of volcanic rocks between Elazığ-Pertek and Kovancilar. *Firat Univ., Faculty Sci. J.*, 1: 9-21. (in Turkish).
- Bingöl A.F., 1984. Geology of the Elazığ area in the eastern Taurus region. In: O. Tekeli and M.C. Göncüoğlu (Eds.), *Proceed. Intern. Symp. Geology of the Taurus Belt*, p. 209-216.
- Bingöl A.F. and Beyarslan M., 1996. Geochemistry and petrology of the Elazığ Magmatics. In: S. Korkmaz and M. Akcay (Eds.), *30th Anniversary Symp. Dept. Geology, Karadeniz Techn. Univ.*, p. 208-227.
- Bölücek, C., Akgül M. and Türkmen I., 2004. Volcanism, sedimentation and massive sulphide mineralisation in a Late Cretaceous arc related basin, Eastern Taurides, Turkey. *J. Asian Earth Sci.*, 24: 349-460.
- Colakoglu A.R., Göncüoğlu M.C., Günay K., Sayit K., Oyan V. and Erdogan K., 2014. Geochemical characteristics and ages of ophiolitic bodies within the East Anatolian Accretionary Complex, NE Van area, E Turkey. *Proceed. 20th. CBGA, Bult. Shkancave Gjeol. Spec. Issue*, p. 20-23.
- Colakoglu A.R., Sayit K., Günay K. and Göncüoğlu M.C., 2012. Geochemistry of mafic dykes from the southeast Anatolian ophiolites, Turkey: Implications for an intra-oceanic arc-basin system. *Lithos*, 132/133: 113-126.
- Dilek Y. and Thy P., 2009. Island arc tholeiite to boninitic melt evolution of the Cretaceous Kızıldağ (Turkey) ophiolite: Model for multi-stage early arc-forearc magmatism in Tethyan subduction factories. *Lithos*, 113 (1): 68-87.
- Humphris S.E. and Thompson G., 1978. Hydrothermal alteration of oceanic basalts by seawater. *Geochim. Cosmochim. Acta*, 42: 107-125.
- Faure G., 2001. *Isotopes: Principles and applications*, 3rd Ed., John Wiley and Sons, USA, 897 pp.
- Faure G. and Mensing T.M., 2005. *Isotopes: Principles and applications*. John Wiley and Sons Inc., 897pp.
- Floyd P.A., Kelling G., Gökçen S.L. and Gökçen N., 1991. Geochemistry and tectonic environment of basaltic rocks from the Misis ophiolitic mélange, South Turkey. *Chem. Geol.*, 89: 263-280.
- Frey F.A. and Weis D., 1995. Temporal evolution of the Kerguelen plume: geochemical evidence from 38 to 82 Ma lavas forming the Ninetyeast Ridge. *Contrib. Mineral. Petrol.*, 121: 12-28.
- Gillis K.M., 1995. Controls on hydrothermal alteration in a section of fast-spreading oceanic crust. *Earth Planet. Sci. Lett.*, 134: 473-489.
- Göncüoğlu M.C., 2014. Comments on a single versus multi-armed Southern Neotethys in SE Turkey and Iran. 3rd Intern. Symp. of IGCP 589 Development of the Asian Tethyan realm. *Abstr. and Proceed.*, p. 89-95.
- Göncüoğlu M.C. and Turhan N., 1984. Geology of the Bitlis Metamorphic Belt. In: O. Tekeli and M.C. Göncüoğlu (Eds.), *Proceed. Intern. Symp. Geology of the Taurus Belt*, p. 237-244.
- Göncüoğlu M.C., Dirik K. and Kozlu H., 1997. General characteristics of pre-Alpine and Alpine Terranes in Turkey: Explanatory notes to the terrane map of Turkey. *Ann. Géol. Pays Hellén.*, 37: 515-536.
- Göncüoğlu M.C., Tekin UK, Sayit K., Bedi Y. and Uzuncimen S., 2015. Opening, evolution and closure of the Neotethyan oceanic branches in Anatolia as inferred by radiolarian research. In: U.K. Tekin and A. Tuncer (Eds.), *Radiolaria. Proceed. INTERRAD*, 35: 88-90.
- Hempton M., 1984. Results of detailed mapping near Lake Hazar Eastern Taurus mountains. In: O. Tekeli and M.C. Göncüoğlu (Eds.), *Proceed. Intern. Symp. Geology of the Taurus Belt*, p. 223-228.
- Hempton M., 1985. Structure and deformation history of the Bitlis suture near Lake Hazar, SE Turkey. *Geol. Soc. Am. Bull.*, 96: 223-243.
- Herece E., Akay E., Kücümün Ö. and Sariaslan M., 1992. Geology of Elazığ-Sivrice and Palu region. General Directorate Mineral Res. Explor. (MTA) Report 9634, 108 pp. (in Turkish, unpublished).
- Karaoglan F., Parlak O., Kloetzli U., Thoeni M. and Koller F., 2013. U-Pb and Sm-Nd geochronology of the Kizildag (Hatay, Turkey) ophiolite: implications for the timing and duration of suprasubduction zone type oceanic crust formation in the southern Neotethys. *Geol. Mag.*, 150 (2): 283-299.
- Köksal S. and Göncüoğlu M.C., 2008. Sr and Nd isotopic characteristics of some S-, I- and A-type granitoids from Central Anatolia. *Turk. J. Earth Sci.*, 17: 111-127.

- Le Maitre R.W., Bateman P., Dudek A., Keller J., Lameyre J., Le Bas M.J., Sabine P.A., Schmidt R., Sorensen H., Streckeisen A., Woolley A.R. and Zanettin B., 1989. A classification of igneous rocks and glossary of terms. Blackwell Sci. Publ.: Recommendations of the international union of geological sciences submission on the systematics of igneous rocks, Oxford, U.K.
- Leat P.T., Livermore R.A., Millar I.L. and Pearce J.A., 2000. Magma supply in back-arc spreading centre Segment E2, East Scotia Ridge. *J. Petrol.*, 41 (6): 845-866.
- Meschede M.A., 1986. Method of discriminating between different types of mid ocean ridge basalts and continental tholeiites with the Nb-Zr-Y diagram. *Chem. Geol.*, 56: 207-218.
- Moghadam H.S., Stern R.J., Chiaradia M. and Mohamad R., 2013. Geochemistry and tectonic evolution of the Late Cretaceous Gogher-Baft ophiolite, central Iran. *Lithos*, 168/169: 33-47.
- Naz H., 1979. The geology of Elazığ-Palu region. *Turk. Petrol. Corp. Rep.*, 1360, 98 pp. (in Turkish, unpublished).
- Nohda S., Tatsumi Y., Yamashita S. and Fujii T., 1992. Nd and Sr isotopic study of Leg 127 basalts: implications for the evolution of the Japan Sea back arc basin. *Proceed. O.D.P. Sci. Res.*, 127/128: 899-904.
- Özkan Y.Z., 1983. A geochemical approach to the origin problem of Caferi Volcanics. *Proceed. Chamber Geol. Engin. Ann. Meetings, Bull. Geol. Congr. Turkey, Ankara*, 4: 53-58.
- Parlak O., Höck V., Kozlu H. and Delaloye M., 2004. Oceanic crust generation in an island arc tectonic setting, SE Anatolian orogenic belt. *Geol. Mag.*, 141: 583-603.
- Parlak O., Rizaoglu T., Bağcı U., Karaoglan F. and Höck V., 2009. Tectonic significance of the geochemistry and petrology of ophiolites in southeast Anatolia, Turkey. *Tectonophysics*, 473: 173-187.
- Pearce J.A., 1983. Role of the sub-continental lithosphere in magma genesis at active continental margins. In: C.J. Hawkesworth and M.J. Norry (Eds.), *Continental basalts and mantle xenoliths*. Shiva Publ., p. 230-249.
- Pearce J.A., 1996. A users's guide to basalt discrimination diagrams. In: D.A. Wyman (Ed.), *Trace Element geochemistry of volcanic rocks: Applications for massive sulphide exploration*. *Geol. Ass. Can., Short Course Notes*, 12: 79-113.
- Pearce J.A., 2008. Geochemical fingerprinting of oceanic basalts with applications to ophiolite classification and the search for Archean oceanic crust. *Lithos*, 100: 14-48.
- Pearce J.A. and Cann J.R., 1971. Ophiolite origin investigated by discriminant analysis using Ti, Zr and Y. *Earth Planet. Sci. Lett.*, 12: 339-349.
- Pearce J.A. and Cann J.R., 1973. Tectonic setting of basic volcanic rocks determined using trace element analyses. *Earth Planet. Sci. Lett.*, 19: 290-300.
- Pearce J.A. and Norry M.J., 1979. Petrogenetic implication of Ti, Zr, Y and Nb variations in volcanic rocks. *Contrib. Mineral. Petrol.*, 69: 33-47.
- Pearce J.A. and Peate D.W., 1995. Tectonic implications of the composition of volcanic arc magmas. *Ann. Rev. Earth Planet Sci.*, 23: 251-285.
- Pearce J.A., Ernewein M., Bloomer S.H., Parson L.M. Murton B.J. and Johnson L.E., 1994. Geochemistry of Lau Basin volcanic rocks: influence of ridge segmentation and arc proximity. In: J.L. Smellie (Ed.), *Volcanism associated with extension at consuming plate margins*. *Geol. Soc. London Spec. Publ.*, 81: 53-75.
- Perincek D., 1979. The geology of Hazro-Korudag-Cüngüs-Maden-Ergani-Hazar- Elazığ-Malatya Area. *Guide Book, Geol. Soc. Turk.*, 33 pp.
- Perincek D. and Kozlu H., 1984. Stratigraphy and structural relations of the units in the Afsin-Elbistan-Dogansehir region (Eastern Taurus). In: O. Tekeli and M.C. Göncüoğlu (Eds.), *Proceed. Intern. Symp. Geology of the Taurus Belt*, p. 181-198.
- Perincek D. and Özkaya I., 1981. Tectonic evolution of the northern margin of Arabian plate. *Bull. Inst. Earth Sci. Hacettepe Univ.*, 8: 91-101.
- Rizaoglu T., Parlak O., Höck V. and Isler F., 2006. Nature and significance of Late Cretaceous ophiolitic rocks and its relation to the Baskil granitoid in Elazığ region, SE Turkey. *Geol. Soc. London Spec. Publ.*, 260: 327-350.
- Rizaoglu T., Parlak O., Höck V., Koller F., Hames W.E. and Billor Z., 2009. Andean type active margin formation in the Eastern Taurides: Geochemical and geochronological evidence from the Baskil Granitoid, SE Turkey. *Tectonophysics*, 473: 188-207.
- Robertson A.H.F., 2002. Overview of the genesis and emplacement of Mesozoic ophiolites in the Eastern Mediterranean Tethyan region. *Lithos*, 65:1-67.
- Robertson A.H.F., 2004. Development of concepts concerning the genesis and emplacement of Tethyan ophiolites in the Eastern Mediterranean and Oman regions. *Earth Sci. Rev.*, 66: 331-387.
- Robertson A.H.F., Parlak O., Rizaoglu T., Ünlügenc U.C., Inan N., Taslı K. and Ustaömer T., 2007. Tectonic evolution of the South Tethyan ocean: evidence from the Eastern Taurus mountains (Elazığ region, SE Turkey). In: A.C. Ries, R.W.H. Butler, and R.H. Graham (Eds.), *Deformation of the continental crust. The legacy of Mike Coward*, *Geol. Soc. London Spec. Publ.*, 272: 231-270.
- Robertson A.H.F., Parlak O. and Ustaömer T., 2013. Late Palaeozoic-Early Cenozoic tectonic development of Southern Turkey and the easternmost Mediterranean region: evidence from the inter-relations of continental and oceanic units. *Geol. Soc. London Spec. Publ.*, 372 (1): 9-48.
- Rollinson H.R., 1993. Discriminating between tectonic environments using geochemical data. In: H.R. Rollinson (Ed.), *Using geochemical data: Evaluation, presentation, interpretation*. Longman Sci. Techn., Essex, UK, p. 171-214.
- Ross P.S. and Bedard J.H., 2009. Magmatic affinity of modern and ancient subalkaline volcanic rocks determined from trace-element discriminant diagrams. *Can. J. Earth Sci.*, 46: 823-839.
- Saunders A.D. and Tarney J., 1984. Geochemical characteristic of basaltic volcanism within back arc basins. In: B.P. Kokelar and M.F. Howells (Eds.), *Marginal basin geology*. *Geol. Soc. London Spec. Publ.*, 16: 59-76.
- Saunders A.D. and Tarney J., 1991. Back-arc basins. In: P.A. Floyd (Ed.), *Oceanic basalts*. Blackie, Glasgow, p. 219-263.
- Sengör A.M.C. and Yilmaz, Y., 1981. Tethyan evolution of Turkey: A plate tectonic approach, *Tectonophysics*, 75: 181-241.
- Shervais J.W., 1982. Ti-V plots and the petrogenesis of modern and ophiolitic lavas, *Earth Planet. Sci. Lett.*, 59: 101-118.
- Sun S.S. and Mc Donough W.F., 1989. Chemical and isotopic systematics of oceanic basalts: implications for mantle composition and processes. In: A.D. Saunders and M.J. Norry (Eds.), *Magmatism in the ocean basins*. *Geol. Soc. London Spec. Publ.*, 42: 313-347.
- Sungurlu O., Perincek D., Kurt G., Tuna E., Dülger S., Celikdemir E. and Naz H., 1985. Geology of the Elazığ-Hazar-Palu area. *Bull. Turk. Ass. Petrol. Geol.*, 29: 83-191.
- Taylor S.R. and McLennan S.M., 1985. The continental crust. Its composition and evolution; an examination of the geochemical record preserved in sedimentary rocks. Blackwell, Oxford, 312 pp.
- Tekin U.K., Ural M., Göncüoğlu, M.C., Arslan M. and Kürüm S., 2015. Upper Cretaceous Radiolarian ages from an arc-backarc within the Yüksekova Complex in the Southern Neotethyan mélange, SE Turkey. *C. R. Palevol.*, 14 (2): 73-84.
- Tian L., Castillo P.R., Hawkins J.W., Hilton D.R., Hanan B.B. and Pietruszka A.J., 2008. Major and trace element and Sr-Nd isotope signatures of lavas from the Central Lau Basin: Implications for the nature and influence of subduction components in the back-arc mantle. *J. Volcan. Geother. Res.*, 178: 657-670.
- Turan M. and Bingöl A. F., 1991. Tectono-stratigraphic characteristics of the region between Kovancilar-Baskil (Elazığ/Turkey). In: C. Yetis (Ed.), *Proceed. Ahmet Acar Geol. Symp.*, Cukurova Univ., Adana, p. 213-227.

- Ural M., Gönçüoğlu M.C., Arslan M., Tekin U.K. and Kürüm S., 2014. Petrological and paleontological evidence for generation of a arc-back arc system within the closing southern branch of Neotethys during the Late Cretaceous. In: A. Begiraj et al. (Eds.), Proceed. 20th CBGA Congr., Bull. Shk. Gjeol. Spec. Issue, 2/2014: 51-54.
- Verma S.P., 2010. Statistical evaluation of bivariate, ternary and discriminant function tectonomagmatic discrimination diagrams. *Turk. J. Earth Sci.*, 19 (2): 185-238.
- Verma S.P. and Agrawal S., 2011. New tectonic discrimination diagrams for basic and ultrabasic volcanic rocks through log-transformed ratios of high field strength elements and implications for petrogenetic processes. *Rev. Mexic. Cienc. Geol.*, 28: 24-44.
- Verma S.K., Pandarinath K. and Verma S.P., 2012. Statistical evaluation of tectonomagmatic discrimination diagrams for granitic rocks and proposal of new discriminant-function-based multidimensional diagrams for acid rocks. *Int. Geol. Rev.*, 54: 325-347.
- Weis D., Kieffer B., Maerschalk C., Pretorius W. and Barling J., 2005. High-precision Pb-Sr-Nd-Hf isotopic characterization of USGS BHVO-1 and BHVO-2 reference materials. *Geochem. Geophys. Geosyst.*, 6.
- Weis D., Kieffer B., Maerschalk C., Barling J., De Jong J., Williams G., Hanano D., Pretorius W., Mattielli N., Scoates J. S., Goolaerts A., Friedman R. and Mahoney J. B., 2006. High-precision isotopic characterization of USGS reference materials by TIMS and MC-ICP-MS. *Geochem. Geophys. Geosyst.*, 7.
- Winchester J.A. and Floyd P.A., 1976. Geochemical magma type discrimination: application to altered and metamorphosed basic igneous rocks. *Earth Planet. Sci. Lett.*, 28 (3): 459-469.
- Winchester J.A. and Floyd P.A., 1977. Geochemical discrimination of different magma series and their differentiation products using immobile elements. *Chem. Geol.*, 20: 325-343.
- Wood D.A., 1980. The application of a Th-Hf-Ta diagram to problems of tectonomagmatic classification and to establishing the nature of crustal contamination of basaltic lavas of the British Tertiary volcanic province. *Earth Planet. Sci. Lett.*, 50: 11-30.
- Woodhead J., Eggins S. and Gamble J., 1993. High field strength and transition element systematics in island arc and back-arc basin basalts: evidence for multi-phase melt extraction and a depleted mantle wedge. *Earth Planet. Sci. Lett.*, 114: 491-504.
- Yazgan E., 1984. Geodynamic evolution of the Eastern Taurus region (Malatya-Elazığ area, Turkey). In: O. Tekeli and M.C. Gönçüoğlu (Eds.), Proceed. Intern. Symp. Geology of the Taurus Belt, p. 199-208.
- Yigitbas E. and Yilmaz Y., 1996. Post-Late Cretaceous strike-slip tectonics and its implications for the Southeast Anatolian orogen, Turkey. *Intern. Geol. Rev.*, 38 (9): 818-831.
- Yilmaz Y., Yigitbas E. and Genc S., 1993. Ophiolitic and metamorphic assemblages of southeast Anatolia and their significance in the geological evolution of the orogenic belt. *Tectonics*, 12 (5): 1280-1297.
- Zindler A. and Hart S., 1986. Chemical geodynamics. *Ann. Rev. Earth Planet. Sci.*, 14: 493-571.

Received, April 4, 2015
Accepted, May 29, 2015